Limits for Metallic Conductivity in Conducting Polymers

R. S. Kohlman,[1] A. Zibold,[2] D. B. Tanner,[2] G. G. Ihas,[3] T. Ishiguro,[4] Y. G. Min,[5]
A. G. MacDiarmid,[5] and A. J. Epstein[1,6]
[1]*Department of Physics, The Ohio State University, Columbus, Ohio 43210-1106*
[2]*Department of Physics, University of Florida, Gainesville, Florida 32611*
[3]*Center for Ultra Low Temperature Research, University of Florida, Gainesville, Florida 32611*
[4]*Department of Physics, Kyoto University, Kyoto 606-01, Japan*
[5]*Department of Chemistry, University of Pennsylvania, Philadelphia, Pennsylvania 19104-6323*
[6]*Department of Chemistry, The Ohio State University, Columbus, Ohio 43210-1106*
(Received 25 July 1996)

The temperature (T) dependent dc conductivity (σ_{DC}) (down to 20 mK) and dielectric function at optical frequencies (0.002–6 eV) and 6.5 GHz are used to probe the inhomogeneous disorder-driven insulator-metal transition in conducting polymers. A correlation between large low T σ_{DC} and the presence to low T of a small fraction of the carrier density delocalized with long transport times ($>10^{-13}$ s) indicates that metallic σ_{DC} is due to only a small fraction of the charge carriers. The achievable σ_{DC} for these systems when the entire charge carrier density participates is estimated to surpass that of copper. [S0031-9007(97)03024-X]

PACS numbers: 71.30.+h, 72.15.Lh, 72.60.+g, 78.66.Qn

The first conducting polymers had modest room temperature (RT) electrical conductivity (σ_{DC}); the T dependence was dominated by variable-range hopping and $\sigma_{\mathrm{DC}} \to 0$ at low T [1,2]. With improved processing [2], σ_{DC} increased appreciably and the strong hopping T dependence was replaced by a much weaker behavior. Indeed, some materials remained metallic even at mK temperatures [3,4]. However, the inhomogeneous morphology [5] of even the most highly conducting samples leads to disorder-induced localization [2,6–11] and percolation effects [7,12] dominating the transport. Because high σ_{DC} is controlled by only the delocalized carrier density in percolating systems [13], by determining the volume density and scattering times (τ) of the delocalized charge carriers, the intrinsic metallic σ_{DC} in conducting polymers can be evaluated. Predictions of anomalously long τ in polymer chains [14] imply that σ_{DC} higher than that of copper conceivably can be obtained if a sufficient fraction of the charge carrier density is delocalized.

Doped polyaniline (PAN) and polypyrrole (PPy) are model systems to study the metallic behavior in anisotropic conducting polymers at low T [2–4,6–9]. Previous RT optical studies of metallic PPy [6] and PAN [7] near an insulator-metal transition (IMT) revealed a negative dielectric function [$\epsilon(\omega)$] in the far infrared at RT, attributed to delocalized carriers with long τ ($\gtrsim 10^{-13}$ s), and an unscreened free carrier plasma frequency $\Omega_p \sim 0.1\ \mathrm{eV} = \sqrt{4\pi\delta ne^2/m^\star}$. Here δ is the fraction of the full carrier density n with long τ, e is the electronic charge, and $m^\star$ is the effective mass [15]. The large majority of the charge carrier density was strongly localized ($\tau \sim 10^{-15}$ s), with unscreened localized charge plasma frequency $\Omega_{p1} \sim 2\ \mathrm{eV} = \sqrt{4\pi ne^2/m_1^\star}$, where $m_1^\star$ is the averaged carrier effective mass. It is noted that a distribution of scattering times is expected in disordered systems. However, this simplified two-fluid model of delocalized and localized carriers demonstrates the essential physics. This inhomogeneous localization of the carrier density is consistent with percolation of a small fraction of the carriers [6–8,12]. It is critical to determine $\epsilon(\omega, T)$ in conjunction with $\sigma_{\mathrm{DC}}(T)$ to understand both T dependent localization of the free carriers near an IMT and whether the full charge carrier density contributes to high σ_{DC} in conducting polymers.

In this Letter, we report the first systematic study of the T dependence of the dielectric function at optical frequencies (2 meV–1 eV) [$\epsilon(\omega)$] and 6.5 GHz (ϵ_{MW}) combined with measurements of $\sigma_{\mathrm{DC}}(T)$ (0.02–300 K) as a function of magnetic field for conducting polymers near an IMT. These data support that the IMT in conducting polymers is due to percolation within an inhomogeneously disordered quasi-1D medium [2,7,8,12]. The data demonstrate directly for the first time the relationship between the percolated free carriers and the metallic σ_{DC} at ~mK in conducting polymers. In particular, for conducting PAN and PPy with high σ_{DC} down to ~20 mK, $\epsilon(\omega, T)$ and $\epsilon_{MW}(T)$ display a Drude response for a small fraction ($\sim 10^{-3}$) of the full carrier density down to low T (~10 K). In contrast, for samples whose $\sigma_{\mathrm{DC}} \to 0$ at mK temperature, the far ir $\epsilon(\omega)$ and $\epsilon_{MW}(T)$ cross over from negative (free carrier) at RT to positive (localized) at low T. A lack of T dependence in $\epsilon(\omega)$ and the absorption coefficient [$\alpha(\omega)$] for the localized majority of carriers ($\tau \sim 10^{-15}$ s) indicates they do not contribute to the high σ_{DC}. Since the high σ_{DC} is controlled by only a small fraction of the total carrier density, substantial increases are expected with improvements in materials.

The conducting PAN samples were doped with *d*,1-camphorsulfonic acid (HCSA) and cast as free standing

films from *m*-cresol [16,17]. PAN-CSA samples A and B were doped by first mixing PAN and HCSA powders and then dissolving them in *m*-cresol while PAN-CSA sample C was prepared by mixing *m*-cresol solutions of PAN and HCSA. The conducting PPy was doped electrochemically with the hexafluorophosphate anion $(PF_6)^-$ [18]. The detailed techniques for measuring σ_{DC} (4.2–300 K) [8], $\epsilon_{MW}(T)$ [8], and the four probe, low frequency (19 Hz) milliKelvin (mK) σ_{DC} [4] were reported earlier. A magnetic field up to 5 T could be applied perpendicular to the plane of the film. The T dependent reflectance was measured using a BOMEM DA3 FTIR spectrometer over 50–10 000 cm^{-1} and a homebuilt Michelson interferometer [19] over 10 – 100 cm^{-1}, both equipped with a continuous flow He cryostat. The high energy (5000–50 000 cm^{-1}) reflectance was measured at RT using a Perkin Elmer Lambda 19 UV/VIS spectrometer equipped with an integrating sphere. The optical dielectric functions were calculated from a Kramers-Kronig analysis [15], as discussed earlier [6]. To calculate the low T $\epsilon(\omega)$, low T reflectance data were extrapolated to higher energy using the RT reflectance.

On the metallic side of an IMT, σ_{DC} is finite [20,21] and the quantity W [$\equiv d\ln\sigma_{DC}(T)/d\ln T$] [20,22] has a positive slope as $T \to 0$. Both PPy-PF_6 and PAN-CSA (A) are on the metallic side of the IMT: $\sigma_{DC} > 170$ S/cm [3] and >70 S/cm, respectively, as $T \to 0$ [Fig. 1(a)] and W has a positive slope [Fig. 1(b)]. For PAN-CSA (A), W has a positive slope even at $T \sim$ mK. Application of a 5 T magnetic field to PAN-CSA (A) increases the mK σ_{DC}, similar to reports for PPy-PF_6 [3,4], and also increases the slope of the mK W plot. Positive magnetoconductance may be due to the effects of weak localization [20,21] and/or enhanced percolation [23]. In contrast, σ_{DC} for PAN-CSA (samples B and C) decreases rapidly with decreasing T with negative slope for the low-T W plot (down to 5 K), characteristic of hopping [$\sigma_{DC} = \sigma_0 \exp(-T_0/T)^\alpha$ [20], where $\alpha \sim 0.3$ and ~ 0.6 for samples B and C, respectively]. For PAN-CSA (B), a crossover in the slope of the low T W plot from negative (insulating) to positive (metallic) with applied magnetic field indicates weak localization effects limit the metallic transport at low T.

The RT $\epsilon(\omega)$ of PPy-PF_6 and PAN-CSA samples A and C (and apparently sample B), Fig. 2, has three zero crossings [6,7]. With decreasing energy, $\epsilon(\omega)$ crosses from positive to negative at ~1 eV, the screened plasma frequency ω_{p1} ($= \Omega_{p1}/\sqrt{\epsilon_C}$ where ϵ_C is the core dielectric constant). Because of localization effects [2,6,7,10,20,21,24], $\epsilon(\omega)$ becomes positive again with decreasing energy. Localization modified Drude model fits indicate a very short "Drude" τ for these localized carriers (~10^{-15} s) [7,10,25]. The low energy (below ~0.03 eV) zero crossing occurs at ω_p ($= \Omega_p/\sqrt{\epsilon_{BG}}$, where ϵ_{BG} includes the screening due to localized carriers), below which $\epsilon(\omega)$ increases to large negative values,

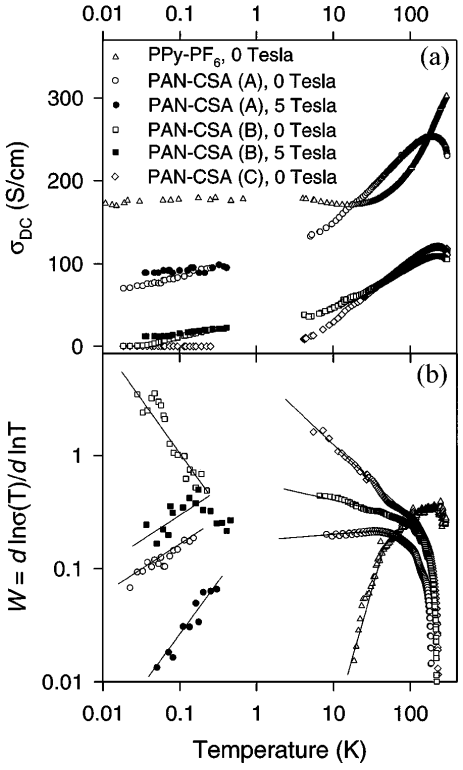

FIG. 1. (a) $\sigma_{DC}(T)$ for PPy-PF_6 and PAN-CSA samples. The mK σ_{DC} for PPy-PF_6 is from Ref. [4]. (b) The reduced activation energy W for PPy-PF_6 and PAN-CSA samples. Inset: The mK W plot for PAN-CSA samples (A) and (B) as a function of magnetic field.

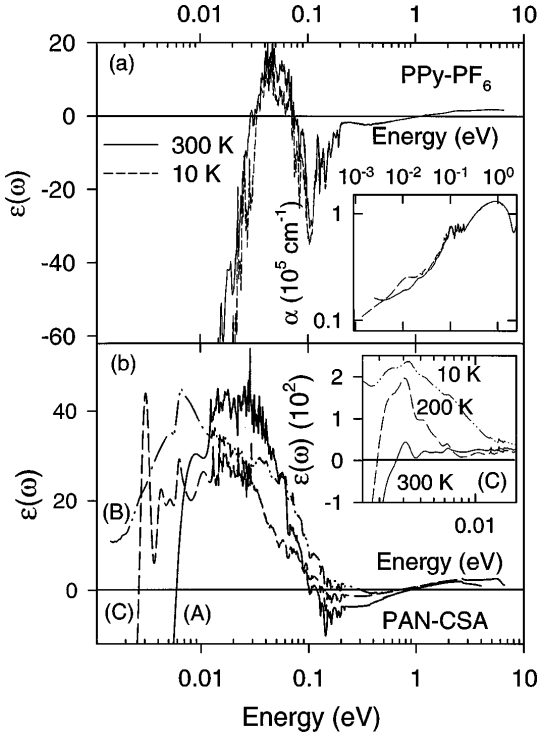

FIG. 2. (a) Comparison of RT $\epsilon(\omega)$ with the 10 K $\epsilon(\omega)$ for PPy-PF_6. Inset: Comparison of the RT and 10 K absorption coefficient for PPy-PF_6. (b) Comparison of the RT $\epsilon(\omega)$ for the PAN-CSA samples. Inset: Comparison of low T and RT $\epsilon(\omega)$ for PAN-CSA (C) which becomes insulating at low T.

characteristic of Drude free carriers [15]. ω_p, Table I, varies approximately with σ_{DC} for each sample.

Comparison of the 10 K ($10-10\,000\ cm^{-1}$) and RT $\epsilon(\omega)$ for PPy-PF_6, Fig. 2(a), shows no T dependence in the vicinity of ω_{p1}, indicating that the associated carriers are strongly localized (confined) by disorder. However, $\epsilon(\omega)$ for energies less than 0.1 eV (free carrier dispersion) demonstrates T dependent localization effects [as in $\sigma_{DC}(T)$] for a fraction of the carriers. Comparison of the RT and 10 K absorption coefficient (α) for PPy-PF_6, inset Fig. 2(a), demonstrates additional absorption due to the charge carriers (pinned mode) localized at low T near $\sim$0.01 eV. The T independence of α in the 0.1–2 eV range again shows that the strongly localized charge carriers do not contribute to the high $\sigma_{DC}(T)$, whereas the weak feature in α near $\sim$0.01 eV is evidence that only a small fraction of the carriers contribute to the high σ_{DC}. Similar experimental behavior was reported for conducting polyacetylene [26].

At high frequency ($\omega\tau > 1$), $\epsilon_{Drude}(\omega) = \epsilon_{BG} - \Omega_p^2/\omega^2$ [15]. The far ir $\epsilon(\omega)$ are linear versus $1/\omega^2$ at each T, Fig. 3, confirming the free carrier behavior and providing $\Omega_p(T)$ from the slopes, Table I. The delocalized fraction (δ) of the charge carrier density can be estimated as $\delta = (m^\star/m_1^\star)(\Omega_p/\Omega_{p1})^2$. Assuming $m^\star \simeq m_1^\star$, $\delta \sim 10^{-3}$, where $\Omega_{p1} \sim 2$ eV for PAN-CSA and PPy-PF_6 [6,7]. It is noted that $m^\star$ may be larger than $m_1^\star$ due to band narrowing in disordered regions. This small δ and $\epsilon(\omega)$ are consistent with metal/insulator composites above the percolation threshold [7,13]. Since the negative far ir $\epsilon(\omega)$ for PAN and PPy show no sign of saturation down to 2 meV, as expected for ϵ_{Drude} when $\omega\tau \leq 1$ [15], τ can be estimated as $\tau > 1/\omega = 1/(2\ meV) \sim 5 \times 10^{-13}$ s. This τ is longer than allowed by the Ioffe-Regel condition for Anderson localization [7].

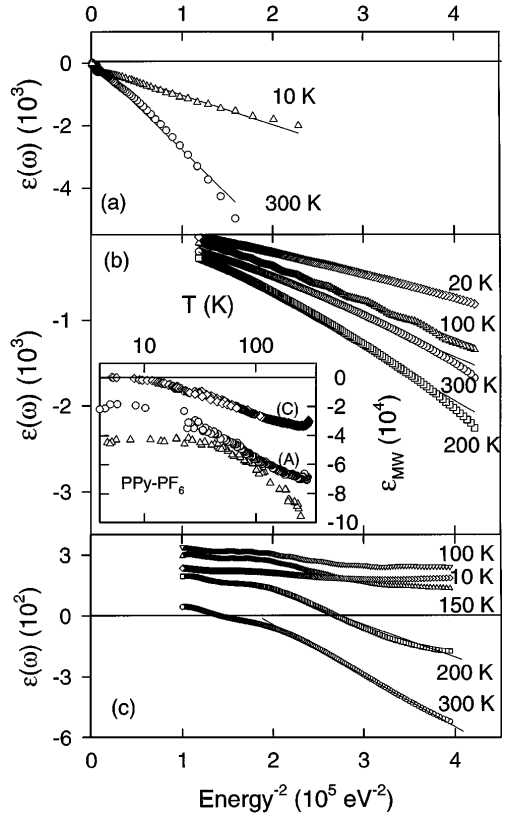

FIG. 3. Comparison of far infrared $\epsilon(\omega)$ at different T showing low frequency Drude behavior for (a) PPy-PF_6, (b) PAN-CSA (A), and (c) PAN-CSA (C). (b) Inset: ϵ_{MW}(T) for PPy-PF_6, PAN-CSA (A), and PAN-CSA (C).

$\epsilon(\omega)$ of metallic PPy-PF_6 and PAN-CSA (A) remains negative in the far ir at low T, Fig. 3, indicating free carriers are present in samples with high σ_{DC} at mK T. However, Ω_p decreases at low T, Table I, consistent with localization of part of the free carrier density at low T, giving rise to a pinned mode as in PPy-PF_6 [Fig. 2(a)]. In contrast, $\epsilon(\omega)$ for PAN-CSA (C) [with $\sigma_{DC} \to 0$ at low T] shows Drude dispersion in the far ir only for $T \gtrsim 150$ K. At $T \sim 150$ K, $\epsilon(\omega)$ is positive in the far ir, indicating a crossover from free carrier diffusion to localization. Therefore, $\Omega_p \to 0$ at low T for insulating PAN-CSA (C) for which $\sigma_{DC} \to 0$ at low T. For samples with $\sigma_{DC}(RT) < 10$ S/cm, $\Omega_p = 0$ even at RT [7].

An estimate of the T dependence of τ can be made using the simple Drude model at low frequency ($\omega\tau \ll 1$) [15], $\sigma_{DC} = \Omega_p^2\tau/4\pi$, together with the experimental $\sigma_{DC}(T)$ and $\Omega_p(T)$ from the optical studies. This analysis ignores the frequency dependence of τ including the effects of localization at low frequency [25]. Because localization effects result in a decrease in σ_{DC}, this provides a low estimate of τ. We obtain $\tau \sim 0.5-6.6 \times 10^{-13}$ s, Table I, approximately the same magnitude estimated from the lack of saturation of $\epsilon(\omega)$, suggesting weak localization effects for the delocalized carriers. The τ at low T are larger than at RT for both PPy-PF_6 and PAN-CSA. The increase of τ at low T is inconsistent with depopulation of extended states with long τ near a mobility edge into localized states with short τ [20,21,24]. However, it could reflect the increased weight of more robust percolation paths with longer τ as less robust paths become localized with decreasing T when phonon-induced delocalization becomes ineffective [2,6–8,12].

ϵ_{MW} [inset Fig. 3(b)] for PPy-PF_6 and PAN-CSA samples (A) and (C) is negative at RT, confirming the

TABLE I. T dependence of the delocalized carrier plasma frequencies and scattering times.

Material	T (K)	σ_{DC} (S/cm)	ω_p (eV)	Ω_p (eV)	τ (10^{-13} s)
PPy-PF_6	300	300	0.03	0.17	0.5
	10	170	0.03	0.1	0.9
PAN-CSA	300	230	0.006	0.07	2.5
(A)	200	250	0.006	0.08	2.0
	100	240	0.006	0.06	2.9
	20	170	0.003	0.05	3.4
PAN-CSA	300	120	0.003	0.04	3.7
(C)	200	120	0.002	0.03	6.6

Drude response at optical frequencies. ϵ_{MW} for metallic PPy-PF_6 and PAN-CSA (A) remains negative down to ~4 K, providing independent confirmation of the presence of free carriers at low T. In contrast, ϵ_{MW} for PAN-CSA (C) decreases in magnitude down to ~10 K, where it crosses from negative (free carriers) to positive (localized carriers), confirming the crossover in the far ir $\epsilon(\omega)$ with decreasing T. However, the crossover in ϵ_{MW} occurs at lower T than for $\epsilon(\omega)$, indicating that the zero crossing of $\epsilon(\omega)$ shifts to lower frequencies as T decreases, consistent with $\Omega_p \rightarrow 0$ at low T.

The presence of free carriers down to low T for PPy-PF_6 and PAN-CSA (A), with large finite σ_{DC} down to ~ mK, in contrast to the absence of free carriers at low T in PAN-CSA (C), which becomes insulating at $T \sim$ mK, identifies the essential role of percolated free carriers in obtaining a metallic σ_{DC}. Potentially large increases in σ_{DC} can be obtained with future improvements in processing that increase the fraction of free carriers from $\delta \sim 10^{-3}$. If the entire carrier density in doped PAN and PPy had a long $\tau \geq 10^{-13}$ s, conductivities in excess of $\sigma_{DC} = \Omega_{p1}^2 \tau / 4\pi \sim (2\ \text{eV})^2 (10^{-13}\ \text{s})/4\pi \geq 10^5$ S/cm would be obtained, comparable with copper. Microwave frequency estimates of $\tau \sim 10^{-11}$ s for some percolated carriers [8] suggest that the intrinsic σ_{DC} for conducting polymers may be higher than copper. Recently, σ_{DC} has been increased for stretched PAN-CSA to $\sim 10^3$ S/cm parallel to the stretch direction [27]. In those stretched PAN-CSA samples, Ω_p parallel to the stretch direction (~0.2 eV) [25] is higher than reported here, confirming that enhanced percolation leads to higher σ_{DC}.

In conclusion, our data support that the IMT in conducting polymers results from a percolation of metallic regions in the presence of inhomogeneous disorder. A conducting polymer on the metallic side of the IMT has a finite σ_{DC} and also a finite density of percolated free carriers as $T \rightarrow 0$. In contrast, for conducting polymers where $\sigma_{DC} \rightarrow 0$ as $T \rightarrow 0$, $\Omega_p \rightarrow 0$ at low T (or even at RT if they have low σ_{DC}). This IMT is not due to a homogeneous decrease of τ for samples near an Anderson IMT but rather results from the loss of percolated electronic paths when phonon-induced delocalization becomes negligible. As only a small fraction of charge carriers ($\delta \sim 10^{-3}$) have percolated Drude behavior in samples studied, substantial increases in σ_{DC} may occur with future improvements in materials.

We thank V. N. Prigodin for useful discussions, and T. Lemberger and R. Rochlin for experimental assistance. This work was supported by NIST ATP 1993-01-0149, NSF DMR-9508723, NSF DMR-9403894, and the University of Florida Division of Sponsored Research.

[1] C. K. Chiang, C. R. Fincher, Jr., Y. W. Park, A. J. Heeger, H. Shirakawa, E. J. Louis, S. C. Gau, and A. G. MacDiarmid, Phys. Rev. Lett. **39**, 1098 (1977).
[2] A. J. Epstein, J. Joo, R. S. Kohlman, G. Du, E. J. Oh, Y. Min, J. Tsukamoto, H. Kaneko, and J. P. Pouget, Synth. Met. **65**, 149 (1994).
[3] T. Ishiguro, H. Kaneko, Y. Nogami, H. Ishimoto, H. Nishiyama, J. Tsukamoto, A. Takahashi, M. Yamaura, T. Hagiwara, and K. Sato, Phys. Rev. Lett. **69**, 660 (1992).
[4] J. C. Clark, G. G. Ihas, A. J. Rafanello, M. W. Meisel, M. Reghu, C. O. Yoon, Y. Cao, and A. J. Heeger, Synth. Met. **69**, 215 (1995).
[5] J. P. Pouget, Z. Oblakowski, Y. Nogami, P. A. Albouy, M. Laridjani, E. J. Oh, Y. Min, A. G. MacDiarmid, J. Tsukamoto, T. Ishiguro, and A. J. Epstein, Synth. Met. **65**, 131 (1994).
[6] R. S. Kohlman, J. Joo, Y. Z. Wang, J. P. Pouget, H. Kaneko, T. Ishiguro, and A. J. Epstein, Phys. Rev. Lett. **74**, 773 (1995).
[7] R. S. Kohlman, J. Joo, Y. G. Min, A. G. MacDiarmid, and A. J. Epstein, Phys. Rev. Lett. **77**, 2766 (1996).
[8] J. Joo, V. N. Prigodin, Y. G. Min, A. G. MacDiarmid, and A. J. Epstein, Phys. Rev. B **50**, 12 226 (1994).
[9] M. Reghu, C. O. Yoon, D. Moses, A. J. Heeger, and Y. Cao, Phys. Rev. B **48**, 17 685 (1993); M. Reghu, Y. Cao, D. Moses, and A. J. Heeger, Phys. Rev. B **47**, 1758 (1993).
[10] K. Lee, A. J. Heeger, and Y. Cao, Phys. Rev. B **48**, 14 884 (1993).
[11] R. Pelster, G. Nimtz, and B. Wessling, Phys. Rev. B **49**, 12 718 (1994).
[12] V. N. Prigodin and K. B. Efetov, Phys. Rev. Lett. **70**, 2933 (1993).
[13] D. J. Bergman and D. Stroud, in *Solid State Physics*, edited by H. Ehrenreich and D. Turnbull (Academic Press, New York, 1992), Vol. 46.
[14] S. A. Kivelson and A. J. Heeger, Synth. Met. **22**, 371 (1988).
[15] F. Wooten, *Optical Properties of Solids* (Academic, New York, 1972).
[16] Y. Cao and A. J. Heeger, Synth. Met. **52**, 193 (1992).
[17] A. G. MacDiarmid and A. J. Epstein, Synth. Met. **65**, 103 (1994).
[18] K. Sato, M. Yamaura, T. Hagiwara, K. Murata, and M. Tokumoto, Synth. Met. **40**, 35 (1991).
[19] K. D. Cummings, D. B. Tanner, and J. S. Miller, Phys. Rev. B **24**, 4142 (1981).
[20] N. F. Mott and M. Kaveh, Adv. Phys. **34**, 329 (1985).
[21] P. A. Lee and T. V. Ramakrishnan, Rev. Mod. Phys. **57**, 287 (1985).
[22] A. G. Zabrodskii and K. N. Zeninova, Zh. Eskp. Teor. Fiz. **86**, 727 (1984) [Sov. Phys. JETP **59**, 425 (1984)].
[23] B. Movaghar and S. Roth, Synth. Met. **63**, 163 (1994).
[24] V. N. Prigodin (private communication).
[25] R. S. Kohlman (unpublished).
[26] H. S. Woo, D. B. Tanner, N. Theophilou, and A. G. MacDiarmid, Synth. Met. **41-43**, 159 (1991).
[27] L. Abell, S. J. Pomfret, E. R. Holland, P. N. Adams, and A. P. Monkman, in *Proc. Soc. of Plastic Engineers Ann. Technical Conf. (ANTEC 1996)* (The Society of Plastic Engineers, Brookville, CT, 1996), p. 1417.